



MAIN ROOF MECHANICAL MODEL AND NUMERICAL SIMULATION OF COMPOSITED BACKFILLING LONG-WALL FACE IN STEEPLY DIPPING COAL SEAM

Wenyu LV^{1,2,3}, Kai GUO³, Yi TAN^{1,2,4}, Xufeng DU³, Ming LIU⁵, Wenjie CAO³

¹ Xi'an University of Science and Technology, State Key Laboratory of Coal Resources in Western China, Xi'an 710054, China

² Henan Polytechnic University, Henan Key Laboratory for Green and Efficient Mining & Comprehensive Utilization of Mineral Resources, Jiaozuo, 454000, China

³ Xi'an University of Science and Technology, School of Energy Engineering, Xi'an 710054, China

⁴ Henan Polytechnic University, School of Energy Science and Engineering, Jiaozuo, 454000, China

⁵ Liaoning Shihua University, School of Mechanical Engineering, Fushun 113001, China

Corresponding author: Wenyu LV, E-mail: lvwenyu@xust.edu.cn

Abstract. The overlying strata movement of steeply dipping coal seam is complicated with large deformation and fracturing of the roof, which often requires the composited backfill mining to effectively improve the stability of surrounding rock. In this paper, the 3221 working face of a test coal mine was taken as the engineering research background. Based on the analysis of the main roof mechanics model of the composited backfilling long-wall face in the steeply dipping coal seam, the finite-difference program FLAC3D and MATLAB were used to numerically study the stress and displacement fields of the main roof under different coal seam dip angles and amounts of artificial waste rock filling. The results showed that as the dip angle increased, the normal force component decreased whereas the tangential force component and the horizontal stress of the roof beam increased. The horizontal displacement increased before the vertical displacement decreased, and the degree of deformation decreased with the increase of the dip angle. The overhanging area of the roof beam reduced with the increase of the filling amount of artificial waste rock, which led to a decreased deformation degree of the roof beam, and the influence on the main roof movement was more obvious than the change of dip angle. The numerical simulation results were found consistent with those from the mechanical model, which proved the rationality of the mechanical model. In general, this research can provide a theoretical basis for the safe and efficient production of the composited backfill mining in steeply dipping coal seams.

Key words: steeply coal seam, composited backfilling, main roof, mechanical model, numerical simulation.

1. INTRODUCTION

The core of safe and efficient mining of the steeply dipping coal seam (SDCS) long-wall face lies in the effective control of the stability of overlying strata[1]. In the long-wall mining process of the SDCS, the characteristics of the roof movement, deformation, and failure in the middle and upper area are active along the inclined direction of the working face, and the contact between the roof and support in this range complicates the loading characteristics, which leads to increased tangential component of gravity and decreased normal component of force with the increase of the dip angle. The support load was not balanced and the working load was reduced [2–3]. The falling of the support and the jamming between the supports can be intensified, causing difficulty to control the stability of the “support-surrounding rock” system and may lead to accidents [4–5]. Although the backfill coal mining method can effectively control the overburden deformation, it reduces the economic benefits of coal mining to a certain extent [6–8]. Considering the fact that the dip angle of the SDCS satisfies the self-slipping condition of the waste rock, the roof beam can be controlled by the composite backfill body of the artificial filling waste rock and caving roof rock. This method can not only make use of the waste rock and reduces filling cost, but it can also

effectively suppress the deformation and failure of the overburden, which is an effective way to realize safe and efficient mining of the SDCS [9].

In recent years, many scholars have analyzed the movement change rules of the roof beam and overlying strata with waste rock filling through mechanical modeling. However, most of the models were based on the elastic theory for beams and thin plates, and the method of fixing beams at both ends was adopted [10–14], whereas the transverse forces on the roof rock beams of the SDCS was not considered. Consequently, the results deviated from the actual situation, and the research on the overburden strata migration rules in the waste rock composited backfilling longwall face were quite few.

Given the above shortcomings, the 3221 working face of a test coal mine was taken as the engineering research background. A mechanical model was established for the main roof displacement deformation of the SDCS long-wall composited backfilling working face, which incorporated the transverse force of the roof beam. By analyzing the movement deformation characteristics of the main roof, the finite-difference program FLAC3D and MATLAB were used to simulate the migration rule of the main roof under different coal seam dip angles and amounts of artificial waste rock filling.

2. ROOF MECHANICAL MODEL OF SDCS LONG-WALL COMPOSITED BACKFILLING FACE

2.1. Development of mechanical model

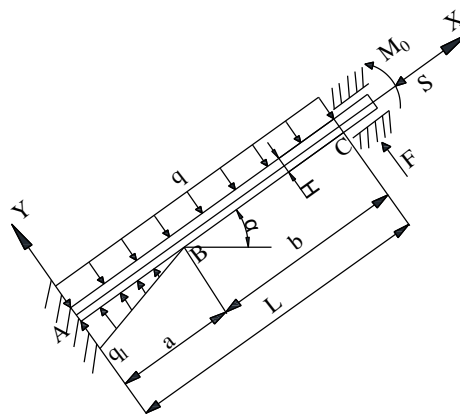


Fig. 1 – Mechanical model of the roof beam.

The 3221 working face of the test coal mine is located at +350m in the upper part of the 322 mining area of the anticline west wing of the Daluowan, the upper part of the working face is the 5614 working face (mined-out), and the south part is the 3222 fully mechanized working face (un-quarried). There was a 1-1 geological drill hole constructed by the original geological prospecting unit reaching this working face. The hole is well sealed with no water gushing out. The strike length of the working face roadway is 246m, the strike length of the airway is 261m, and the dip length is about 105m. The dip angle is $36^\circ \sim 42^\circ$ with an average of 40° . The coal seam generally has a simple structure. The overall coal seam structure is 0.18 (0.22) 0.98 (0.26) 0.18 (0.07) 1.70, and the full height of the coal seam is 3.07m \sim 3.56m, the average full height is about 3.43m. In the actual production of the 3221 SDCS longwall working face, support toppling and sliding are intensified and the roof movement in the middle and upper area is active, which is prone to spalling and roof falling. At present, the working face mainly adopts the full caving method to manage the roof, which uses the methods of moving the support under pressure to improve the actual initial support force and working resistance of the support, and by adding anti-skid Jack to improve the roof support efficiency and the stability of the support-surrounding rock system.

The proposed mechanical model of the roof beam has assumed: Euler beam, fully elastic, and small strain. In Fig. 1, as the depth of the coal seam is a lot greater than the vertical projection of the work face, the load from the overlying strata was assumed to have $q = \gamma Y_a \cos \alpha$, the coal seam dip angle is α , the working face length is L , the roof thickness is H , the elastic modulus is E , the coal mass moment of inertia is I , the

bulk density is γ , the buried depth is Y_a , the coal seam burial s taken as the X axis, and the direction perpendicular to the roof upward is taken as the Y axis. The rectangular coordinate system AXY is established. Since the depth of the coal seam is greater than the projection of the working face length in the vertical direction, for convenience, the axial force is defined as $S = \gamma Y_a H \sin \alpha$. The caved immediate roof in the middle and lower parts of the working face shows triangular area, and its load satisfies triangular distribution characteristics, corresponding to the load q , that $q_1 = q$. According to the mechanical model in Fig. 1, it can be seen from the bending moment theory in material mechanics that:

– The differential equation of the deflection line of roof rock beam AB can be expressed as:

$$y''_{AB}(x) = \frac{M_0}{EI} + \frac{F}{EI}(L-x) - \frac{S}{EI}y_{AB}(x) - \frac{q}{2EI}(L-x)^2 + \frac{1}{EI} \int_x^a q \frac{a-\eta}{a}(\eta-x)d\eta \quad 0 \leq x < a; \tag{1}$$

– The differential equation of the deflection line of roof rock beam BC can be expressed as:

$$y''_{BC}(x) = \frac{M_0}{EI} + \frac{F}{EI}(L-x) - \frac{S}{EI}y_{BC}(x) - \frac{q}{2EI}(L-x)^2 \quad a \leq x < L, \tag{2}$$

where F, S and M_0 are shear force, axial force and nodal bending moment at the body C in the upper part of the working face, respectively. According to the force characteristics and constraint conditions AB , the corresponding boundary conditions are as below:

$$y_{AB}(0) = 0, \theta_{AB}(0) = 0, y_{BC}(L) = 0, \theta_{BC}(L) = 0, y_{AB}(a) = y_{BC}(a), \theta_{AB}(a) = \theta_{BC}(a).$$

– The equations of deflection and rotation of AB and BC sections of the roof rock beams are:

$$y_{AB}(x) = C_1 \cos \sqrt{\frac{S}{EI}}x + C_2 \sin \sqrt{\frac{S}{EI}}x + \left(\frac{2Lq - 2F - aq}{2S} \right)x + \frac{EIq}{aS^2}x - \frac{q}{6aS}x^3 + \frac{M_0}{S} + \frac{FL}{S} + \frac{a^2q - 3L^2q}{6S} \tag{3}$$

$$y_{BC}(x) = C_3 \cos \sqrt{\frac{S}{EI}}x + C_4 \sin \sqrt{\frac{S}{EI}}x - \frac{q}{2S}x^2 + \left(\frac{qL - F}{S} \right)x + \left(\frac{M_0}{S} + \frac{FL}{S} - \frac{FL^2}{2S} + \frac{EIq}{S^2} \right) \tag{4}$$

$$\theta_{AB}(x) = -C_1 \sqrt{\frac{S}{EI}} \sin \sqrt{\frac{S}{EI}}x + C_2 \sqrt{\frac{S}{EI}} \cos \sqrt{\frac{S}{EI}}x - \frac{q}{2aS}x^2 + \frac{EIq}{aS^2} - \frac{F}{S} + \frac{Lq}{S} - \frac{aq}{2S} \tag{5}$$

$$\theta_{BC}(x) = -C_3 \sqrt{\frac{S}{EI}} \sin \sqrt{\frac{S}{EI}}x + C_4 \sqrt{\frac{S}{EI}} \cos \sqrt{\frac{S}{EI}}x - \frac{qx - qL + F}{S}. \tag{6}$$

According to the above analysis, E, I, q, S, a, L are constants, $C_1, C_2, C_3, C_4, F, M_0$ are unknowns, which can be expressed as:

$$\begin{bmatrix} 1 & 0 & 0 & 0 & \frac{1}{S} & \frac{L}{S} \\ 0 & \sqrt{\frac{S}{EI}} & 0 & 0 & 0 & -\frac{1}{S} \\ 0 & 0 & \cos \sqrt{\frac{S}{EI}}L & \sin \sqrt{\frac{S}{EI}}L & \frac{1}{S} & -\frac{L^2}{2S} \\ 0 & 0 & -\sqrt{\frac{S}{EI}} \sin \sqrt{\frac{S}{EI}} & \sqrt{\frac{S}{EI}} \cos \sqrt{\frac{S}{EI}}L & 0 & -\frac{1}{S} \\ \cos \sqrt{\frac{S}{EI}}a & \sin \sqrt{\frac{S}{EI}}a & -\cos \sqrt{\frac{S}{EI}}a & -\sin \sqrt{\frac{S}{EI}}a & 0 & \frac{L^2}{2S} \\ -\sqrt{\frac{S}{EI}} \sin \sqrt{\frac{S}{EI}}a & \sqrt{\frac{S}{EI}} \cos \sqrt{\frac{S}{EI}}a & \sqrt{\frac{S}{EI}} \sin \sqrt{\frac{S}{EI}}a & -\sqrt{\frac{S}{EI}} \cos \sqrt{\frac{S}{EI}}a & 0 & 0 \end{bmatrix} \begin{bmatrix} C_1 \\ C_2 \\ C_3 \\ C_4 \\ M_0 \\ F \end{bmatrix} = \begin{bmatrix} \frac{3L^2q - a^2q}{6S} \\ \frac{aq}{2S} - \frac{EIq}{aS^2} - \frac{qL}{S} \\ -\frac{L^2q}{2S} - \frac{EIq}{S^2} \\ 0 \\ \frac{L^2q}{2S} \\ -\frac{EIq}{aS^2} \end{bmatrix} \tag{7}$$

2.2. Mechanical model analysis

Based on the characteristics of the non-uniform filling and non-symmetrical constraint in the SDCS longwall mining, the migration rule of the overburden strata would also change under different coal seam dip angles and amounts of the artificial waste rock filling. By fixing other variables, the deflection and rotation of different coal seam dip angles and artificial filling amounts were analyzed. According to the engineering conditions, the elastic modulus of the roof beam E is 10 GPa, the inertia moment of the roof beam I is 83 m⁴, the working face length L is 200 m, the width of roof beam H is 15 m, the bulk density γ is 25 KN/m³, the coal seam dip angle α is 45°, and the buried depth Y_a is 300 m.

(1) Different coal seam dip angles

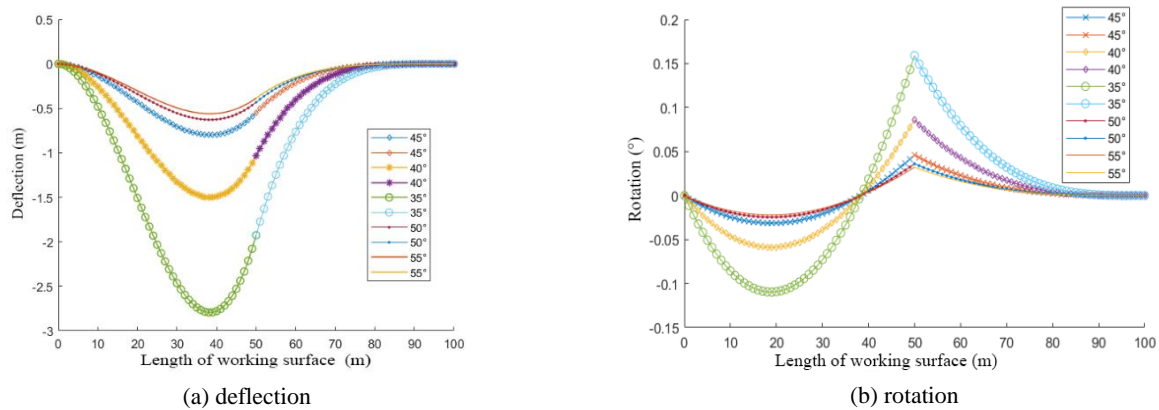


Fig. 2 – Variations of roof deflection and rotation under different coal seam dip angle.

As shown in Fig. 2, for different working face dip angles (35°, 40°, 45°, 50°, 55°), artificial waste rock filling was conducted for the SDCS. The caved roof rock slipped towards the lower area of the goaf, resulting in the unbalanced filling effect of lower filling compacting, a middle loose filling, and upper suspension. The displacement deformation and failure characteristics of the roof in the middle and upper area along the inclined direction of working face were obvious. The contact between the roof and the support in this range made the loading characteristics complicated, and the tangential component of gravity increased while the normal component of force decreased with the increase of the dip angle, and the displacement deformation also decreased. Under the constraint of the waste rock backfilling, the deflection of roof rock beam was larger at the middle position than at the upper and lower positions, due to the inclination effect of coal mining. The rotation of the roof beam showed a trend of first increasing, then decreasing, and then increasing in the AB section, reaching the maximum at point B and showing a decreasing trend in the BC section. With the increase of the dip angle, the deflection and rotation of the roof beam decreased, and the gap decreased gradually.

As our study is mainly concerned with coal seams with large dip angles (35°–55°), the variation of S is relatively small and thus demonstrating insignificant effect on the overall results.

(2) Different filling amounts of artificial waste rock

In this study, the artificial filling was considered as dense filling. In order to facilitate the calculation of mechanical model, the artificial filling was removed and only retained as the length of filling section, that is, the change of artificial gangue filling length is equivalent to the change of the working face length in the mechanical model. The effect of backfilling amount has been analyzed by assuming constant dip angle and S . It can be seen from Fig. 3 that for different working face lengths (80, 100, 120, and 140 m), the suspended area of the roof increased and the moving deformation and failure intensified, with the reduction of artificial waste rock amounts. From the figure when the working face length was greater than 100 m, the deflection of the AB section and BC section of roof rock beams all increased first and then decreased. When the working face was less than 100 m, the rotation of the roof beam was generally larger in the middle than in the upper

and lower parts. The rotation of the roof beam first showed an increasing trend, then decreasing, and finally increasing in the *AB* section. It reached its maximum at point *B* and showed a trend of first decreasing, then increasing and finally became decreasing in section *BC*, which was contrary to section *AB*. With the increase of the amount of the artificial waste rock, the influence of the change of the working face length was greater than that of the dip angle of the coal seam, and its influence on the roof migration of the composited backfilling of the SDCS was more obvious.

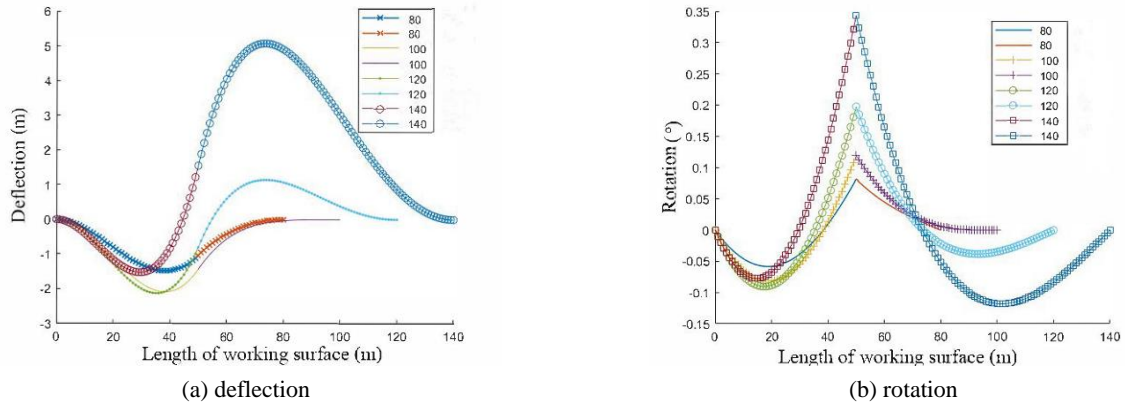


Fig. 3 – Deflection and rotation of roof beam under different artificial waste rock backfilling amounts.

The proposed mechanical model is for the purpose of qualitative analysis, which cannot be compared quantitatively with the following numerical results.

3. NUMERICAL EXPERIMENT

3.1. Establishment of numerical model

Table 1

Geometrical and mechanical parameters of the model

Rock name	Bulk density [kg/m ³]	Bulk modulus [GPa]	Shear modulus [GPa]	Poisson's ratio	Compressive strength [MPa]	Adhesion [MPa]	Friction angle [°]
Coarse sandstone	2350	5.0	3.7	0.09	26	2.1	30
Sandstone	2350	4.2	3.0	0.23	34	4.9	28
Fine sandstone	2510	9.3	9.1	0.25	22	2.0	27
Siltstone	2640	9.3	3.7	0.13	25	3.0	26.5
Medium sandstone	2510	4.2	3.1	0.09	20	2.0	29.5
Mudstone	2530	4.1	3.7	0.10	21	2.1	28
Sandy mudstone	2350	5.0	2.9	0.23	34	4.9	27.5
Calcareous mudstone	2510	4.2	1.0	0.11	20	2.2	23
Coal seam	1440	1.5	3.0	0.30	6	1.0	28
Carbonaceous Mudstone	2510	4.2	1.8	0.09	20	2.0	26
Bauxite	2369	2.8	3.7	0.21	21	3.4	28
Limestone	2350	5.0	5.0	0.23	34	4.9	27.5
Coarse sandstone	2350	5.0	3.7	0.09	26	2.1	30

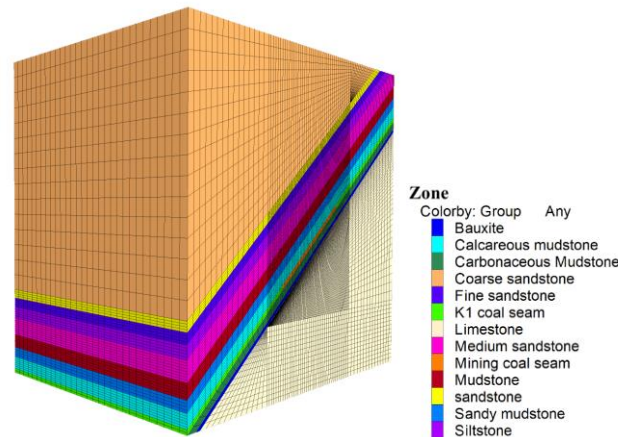


Fig. 4 – Illustration of the numerical model for the studied work face.

The basic numerical computational mechanical model was established according to the geological condition of the 3221 working face using the constitutive model of the built-in Mohr-Coulomb plasticity model in FLAC3D. [15–16]. The dimension of the basic model was 300 m×240 m×300 m. To better mimic the actual engineering conditions, the physical and mechanical parameters of coal seam and main rock strata were obtained according to geological data and laboratory rock mechanics experiment results. The geometrical and mechanical parameters of the model were shown in Table 1.

The basic dimensions of the model were as follows: coal seam mining height was 3.2 m, working face length was 105 m except for artificial waste rock, and dip angle was 40°. The entire model was composed of 936,870 units, which include 965,705 nodes, as shown in Fig. 4.

The long-wall face mining method was adopted in the model in the process backfilling. To reduce the boundary effect, coal pillars of 100 m wide were placed at both sides of the work face so that there is no plastic failure penetrating to the boundary. The bottom boundary was set with no vertical movement, and the side boundaries were set with no horizontal movement. The horizontal movement was restricted by the front, rear, and left sides of the model. To be more realistic, a load of 8MPa was also set at the top boundary. Stress balance was achieved by running the model once before the excavation. Due to a large number of nodes in the simulations, the excavation step was set as 20 m, the filling process was modeled by redefining the volume properties according to the infilling properties after excavation.

3.2. Results of numerical simulations

(1) **Roof movement rule under different coal seam dip angles.** Under different coal seam dip angles, the displacement and stress variation characteristics of the main roof were analyzed under the working conditions of 3.2 m mining height, 105 m working face length, and 1/3 of the filling face length of waste rock along the lower end of the coal seam.

① Vertical displacement characteristics of the main roof

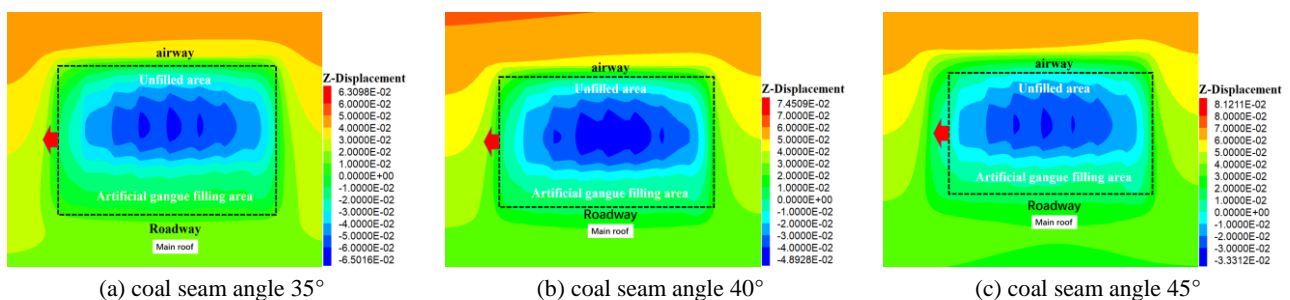


Fig. 5 – Changes in vertical displacement [m] of the main roof of different coal seams dip angles.

It can be seen from Fig. 5 that due to artificial waste rock and caved rock filled to mined-out areas, the exposed space of goaf was reduced, the contact area between backfilling body and roof was increased, and the displacement of the main roof was restrained to a great extent. The change of vertical displacement in the filling area of 1/3 waste rock at the bottom of the main roof decreased obviously. The maximum displacement of the main roof occurred in the middle and upper parts of the working face. When the working face advanced 160 m and the dip angle of the coal seam was 35°, the largest vertical displacement of the main roof was 65.02 mm. When the dip angle of the coal seam was 40°, the largest vertical displacement of the main roof was 48.93 mm; when the dip angle of the coal seam was 45°, the largest vertical displacement was 33.31 mm. Due to the increase of coal seam dip angle, the waste rock was more likely to fall to the lower part after entering the goaf, which increased backfill density to control rock strata movement. The displacement of surrounding rock decreased, which caused the vertical displacement of the main roof, however, the reduction amplitude was decreased.

② Vertical stress characteristics of the main roof along the strike direction

From Fig. 6, it can be seen that the concentrated stress in the main roof stress concentration area significantly decreased. The stress transferred from the immediate roof to the main roof decreased obviously. The stress concentration area was distributed around the working section. When the working face advanced 160m and the dip angle of the coal seam was 35°, the largest concentrated stress was 14.52 MPa and the maximum stress value in the stress release area was 0.090 MPa; When the dip angle of the coal seam was 40°, the largest concentrated stress was 14.06 MPa and the maximum stress value in the stress release area was 0.087 MPa; When the dip angle of the coal seam was 45°, the largest concentrated stress was 12.97 MPa and the maximum stress value in the stress release area was 0.082 MPa. After mining, the roof strata were often bent under the action of weight stress and overlying strata compressive stress. When the deformation reached a certain degree, the caving rock entered the goaf. Therefore, the component force of rock towards goaf was directly related to the level of surrounding rock deformation and failure. With the increase of coal seam dip angle, the component force of gravity of roof and overlying strata towards goaf decreased continuously, the stress concentration degree decreased and the reduction amplitude increased gradually.

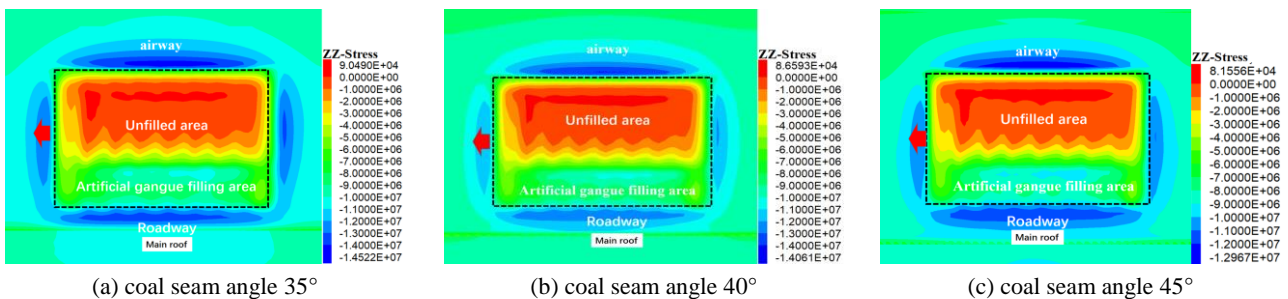


Fig. 6 – Changes in the vertical stress [Pa] of different coal seams dip angles.

③ Characteristics of the plastic zone of the main roof

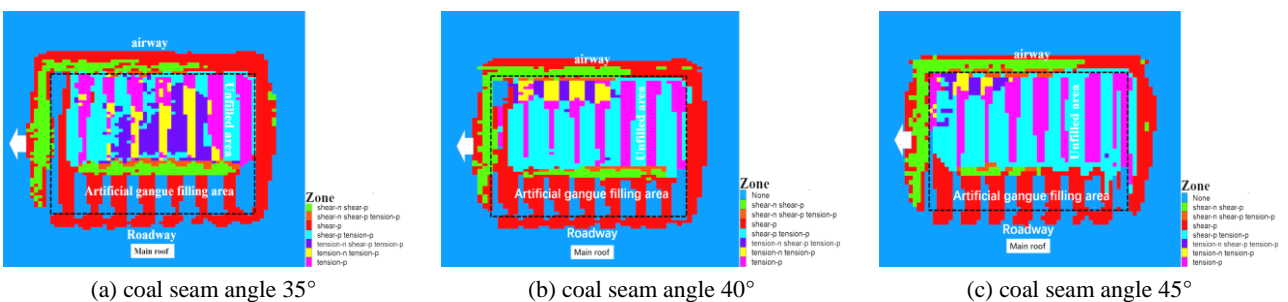


Fig. 7 – Main roof failure field with different coal seam dip angles.

It can be seen from Fig. 7 that with the increase of the dip angle of the coal seam, the plastic zone of the main roof decreased significantly. Shear failure mainly occurred around the working section and the plastic zone of the main roof of filling area. The distribution characteristics of the plastic zone of the main roof with different coal seam dip angles were the same.

(2) **Roof migration rules under different artificial waste rock filling amounts.** Under different artificial waste rock filling amounts, the displacement, stress, and plastic zone characteristics of the main roof were analyzed with a coal seam dip angle of 40° , working face mining height of 3.2 m, and 105 m working face length.

① *Vertical displacement characteristics of the main roof*

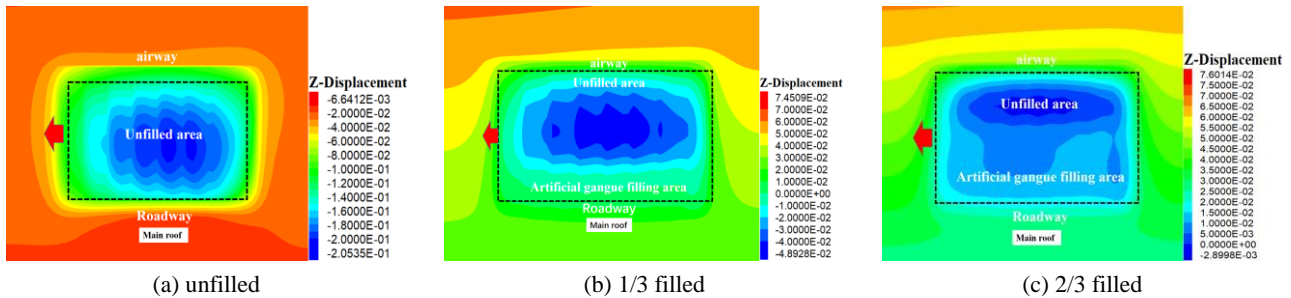


Fig. 8 – Vertical displacement [m] of the main roof under different artificial waste filling amounts.

From Fig. 8, it can be seen that the vertical displacement of the main roof was significantly reduced compared to the cases when different artificial waste rock filling amounts. Main roof subsidence only occurred in the unfilled area, and the subsidence displacement decreased gradually in a step-shaped manner in the middle of the unfilled area. In the area outside the working section, the upward displacement increased gradually from the lower part to the upper part of the working face, and more artificial waste filling amount led to smaller displacement. When the working face was forward 160 m and not adopt backfilling method, the largest main roof subsidence displacement was 205.35 mm; when the artificial waste filling amount was 1/3, the largest main roof subsidence displacement was 48.93 mm; when the artificial waste filling amount was 2/3, the largest main roof subsidence displacement was 2.90mm. When using the backfilling method, the vertical displacement of the main roof was further reduced by the support of the artificial waste rock and the immediate roof structure. With the increase of artificial waste rock filling amount, the movement space of surrounding rocks in goaf was smaller, which had an obvious influence on the subsidence displacement of the main roof of the working section, while it showed little influence on the area outside the working section.

② *Vertical stress characteristics of the main roof*

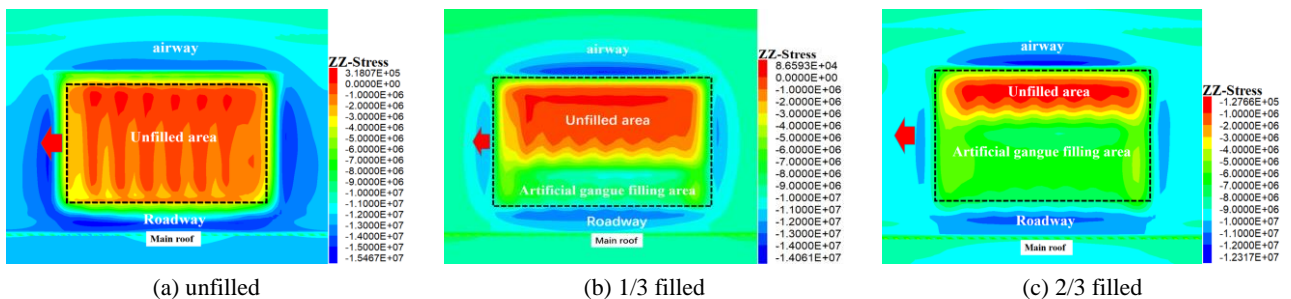


Fig. 9 – The vertical stress [Pa] of the main roof of different artificial waste filling amounts.

It can be seen from Fig. 9 that the vertical stress variation diagram of the main roof forward by different artificial waste rock filling amounts, the main roof stress concentration value decreased, and there was no obvious stress concentration phenomenon in the upper roof of the waste rock filling area. When the

working face was forwarded 160 m without backfilling, the largest main roof vertical stress was 15.47 MPa, and the largest main roof vertical stresses of 14.06 MPa and 12.32 MPa occurred at the upper part of the filling area at the artificial waste rock filling amounts of 1/3 and 2/3, respectively. Thus, it can be observed that artificial waste rock filling amounts can change the position of maximum supporting stress in the filling area of waste rock. With the increase of artificial waste rock filling amount, the vertical stress of the main roof gradually decreased. When the waste rock was filled into the goaf, the working section become stable, the surrounding rocks slowly moved into the goaf, and the waste rock gradually supported the roof and floor, so that the stress of the surrounding rocks can be partially transferred, then forming the stress recovery zone and reducing the range of the stress relief zone.

③ Characteristics of the plastic zone of the main roof

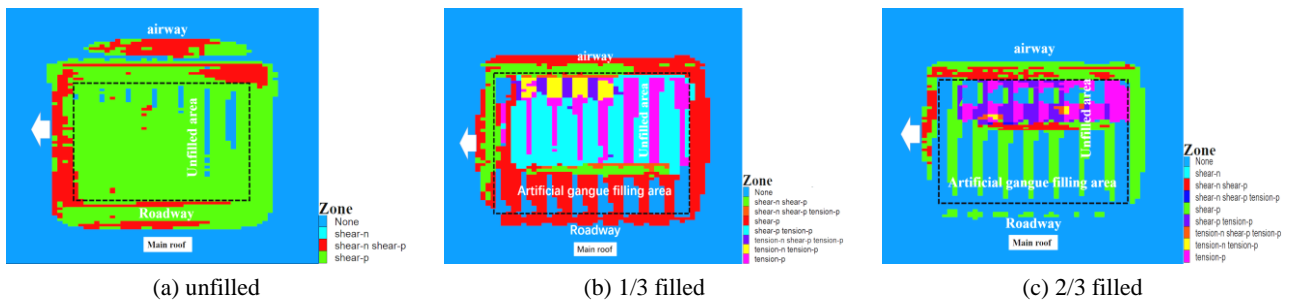


Fig. 10 – Main roof failure field with different artificial waste filling amounts.

It can be seen from Fig. 10 that larger artificial waste rock filling amounts would change the original goaf form and reduce the exposed space from the failure field of the main roof. The movement mode of the roof and floor was changed, and the space for bending deformation of the roof became smaller. The stress in the rock mass cannot be released, which weakened the scope and degree of the roof strata fracture and failure. Only shear failure occurs in the filling area. The coal wall and pillar around the working section were damaged by shear, the coal pillar failure range on the working face was larger than that on the lower face, and the increase of the waste rock filling amounts would decrease the failure range.

4. CONCLUSIONS

The following conclusions can be drawn from this study:

1) The mechanical model of the main roof using the composited backfill mining in the SDCS was established. With the increase of the dip angle and filling amount of the artificial waste rock, the deflection and rotation of the roof beam decreased continuously, whereas the gap decreased gradually. It was found that the change of the filling amount of artificial waste rock demonstrated an obvious influence on the migration of the main roof of the SDCS mining. Despite its insignificant influences in this study, the effect of shear deformation should be incorporated into the mechanical model for more complex situations. This will be covered in our subsequent studies.

2) The numerical simulation results suggested that the larger the artificial waste rock filling amount was, the smaller the vertical stress and vertical displacement of the main roof were with less evident impact. However, the influence on the area outside the working section was not significant, and the plastic zone decreased gradually. With the increase of the dip angle of the coal seam, the tangential stress of the roof increased, whereas the normal phase stress decreased, the vertical displacement of the main roof decreased, and the degree of deformation and failure decreased.

3) It was shown that the numerical simulation results agreed qualitatively with the model calculation results, and the model demonstrated higher rationality, which may provide a theoretical basis for the study of the overburden strata migration rule in the SDCS mining.

ACKNOWLEDGMENTS

This study was financially supported by the National Natural Science Foundation of China (No. 51974226, 52174127, 51634007), the Research Fund of Henan Key Laboratory for Green and Efficient Mining & Comprehensive Utilization of Mineral Resources (Henan Polytechnic University, No. KCF202001), the Research Fund of Shaanxi Key Laboratory of Coal Mine Water Disaster Prevention and Control Technology (No. 2020SKMS02) and the Research Fund of State Key Laboratory of Coal Resources in Western China (No. SKLCRKF1912).

REFERENCES

1. P.S. XIE, Y. LUO, Y.P. WU, X.C. GAO, S.H. LUO, Y.F. ZENG, *Roof deformation associated with mining of two panels in steeply dipping coal seam using subsurface subsidence prediction model and physical simulation experiment*, *Mining Metall Explor.*, **37**, 2, pp. 581–591, 2020.
2. P.S. XIE, Y.P. WU, *Deformation and failure mechanisms and support structure technologies for goaf-side entries in steep multiple seam mining disturbances*, *Arch Min Sci.*, **64**, 3, pp. 561–574, 2019.
3. Y.P. WU, B.S. HU, D. LANG, Y.P. TANG, *Risk assessment approach for rockfall hazards in steeply dipping coal seams*, *Int J Rock Mech Min.*, **138**, p. 104626, 2021.
4. C.F. HUANG, Q. LI, S.G. TIAN, *Research on prediction of residual deformation in goaf of steeply inclined extra-thick coal seam*, *Plos One*, **15**, 10, p. e0240428, 2020.
5. J.A. WANG, J.L. JIAO, *Criteria of support stability in mining of steeply inclined thick coal seam*, *Int J Rock Mech Min.*, **82**, pp. 22–35, 2016.
6. X.Z. WANG, J.L. XIE, J.L. XU, W.B. ZHU, L.M. WANG, *Effects of coal mining height and width on overburden subsidence in longwall pier-column backfilling*, *Appl Sci.*, **11**, p. 3105, 2021.
7. W.B. LIU, J.M. XU, W.B. ZHU, S.H. WANG, *A novel short-wall caving zone backfilling technique for controlling mining subsidence*, *Energy Sci. Eng.*, **7**, pp. 2124–2137, 2019.
8. B. LU, Y.L. LI, S.Z. FANG, H. LIN, Y. ZHU, *Cemented backfilling mining technology for gently inclined coal seams using a continuous mining and continuous backfilling method*, *Shock Vib.*, p. 6652309, 2021.
9. W.Y. LV, Y.P. WU, M. LIU, J.H. YIN, *Migration law of the roof of a composited backfilling longwall face in a steeply dipping coal seam*, *Minerals*, **9**, 3, p. 188, 2019.
10. Q.L. CHANG, J.H. CHEN, H.Q. ZHOU, J.B. BAI, *Implementation of paste backfill mining technology in Chinese coal mines*, *Sci. World J.*, **82**, p. 1025, 2014.
11. J.L. XIE, W.B. ZHU, J.L. XU, J.H. WEN, C. LIU, *A study on the bearing effect of pier-column backfilling in the goaf of a thin coal seam*, *Geosci. J.*, **20**, 3, pp. 361–369, 2016.
12. W.Y. QI, J.X. ZHANG, N. ZHOU, Zhongya WU, Jun ZHANG, *Mechanism by which backfill body reduces amount of energy released in deep coal mining*, *Shock Vib.*, p. 8253269, 2019.
13. H. PU, J. ZHANG, *Research on protecting the safety of buildings by using backfill mining with solid*, *Procedia Environ. Sci.*, **12**, Part A, pp. 191–198, 2012.
14. P.F. ZHANG, T.B. ZHAO, Z.Y. FU, X. TIAN, D. QIU, *Analysis on roof subsidence law and gangue load bearing characteristics in gangue filling goaf*, *Coal Sci Technol.*, **46**, 11, pp. 50–56, 2018.
15. X. D. ZHAO, J. JIANG, B.C. LAN, *An integrated method to calculate the spatial distribution of overburden strata failure in longwall mines by coupling GIS and FLAC3d*, *Int. J. Min. Sci. Technol.*, **25**, 3, pp. 369–373, 2015.
16. R. WU, J.H. XU, C. LI, Z.L. WANG, S. QIN, *Stress distribution of mine roof with the boundary element method*, *Eng Anal Bound Elem.*, **50**, pp. 39–46, 2015.

Received January 5, 2021